HARMONIC DISTURBANCE REJECTION CONTROL FOR MAGNETIC FIELD COMPENSATION APPLICATIONS

G. O. FORTE and E. ANOARDO

†*LaRTE, Grupo de Resonancia Magnética Nuclear, Facultad de Matemática Astronomía y Física, Universidad Nacional de Córdoba and IFEG (CONICET), Argentina.*
forte@famaf.unc.edu.ar, anoardo@famaf.unc.edu.ar

***Abstract*— A simple control strategy was studied for harmonic disturbance rejection in magnetic field compensation systems for low-field magnetic resonance techniques. The strategy is based on the simultaneous action of a conventional PID and a selective harmonic-compensation controller. The system consists of a set of compensating coils fed by independent current sources driven by a digital controller. A series of hall magnetic sensors close the control loop. Despite its simplicity, it is shown that the performance of the dual controller improves within the frequency range where the waterbed effect becomes dominant, by selectively enhancing the rejection of the harmonic component. The proposed solution is particularly useful for selective harmonic rejection of slowly varying frequency and amplitude dependent harmonic perturbations. An extension to multiple-harmonic components perturbations is possible.**

***Keywords*— Automatic frequency control, waterbed effect, harmonic rejection, periodic control.**

I. INTRODUCTION

Field-cycling nuclear magnetic resonance (NMR) techniques require magnetic field compensation in order to run experiments at very low or zero-field conditions (Anoardo and Ferrante, 2003). In NMR relaxometry applications, it is desirable to extend the operative magnetic field range of the hardware in order to scan relaxation parameters up to very weak magnetic fields (Kimmich and Anoardo, 2004). A magnetic field compensator is also atractive for Zero-field NMR spectroscopy and double resonance nuclear quadrupole spectroscopy (NQR) as well. More recently, field-cycling magnetic resonance imaging (MRI) has been performing as a new paradigm of potential massive use in medical diagnosis (Lurie *et al.*, 1998; Matter *et al.*, 2006). For all of these, a quality compensation of the magnetic field not only demands for cancellation of time-independent components, but also for time-dependent and harmonic contributions arising from the environment.

The problem is more general however. There are many applications where the attenuation or cancelation of periodic disturbances are necessary. Active shielding (Kuriki *et al.*, 2002; Platzek *et al.*, 1999; Sergeant *et al.*, 2003; Sergeant *et al.*, 2007; ter Brake *et al.*, 1993) and active noise cancellation (Kuo and Morgan, 1999; Nelson and Elliot, 1992) are examples. The problem of rejecting periodic disturbances with uncertain frequency is common in mechanical and electronic systems. Different solutions were considered, as for example, adaptive algorithms to estimate the frequency and the amplitude of the disturbance in combination with a phase-locked loop (Bodson and Douglas, 1997) or, internal model (IM)-based adaptive algorithms (Brown and Qing Zhang, 2004).

In most cases, the solution is based on controllers operating in the time domain. In the case of a noise perturbation composed of several frequency components, those within the bandwidth of the controller will be attenuated, while those occurring at higher frequencies will be amplified; phenomena called "waterbed effect" (Skogestad and Postlethwaite, 2005). If these last components can be selectively mitigated by other means, it would be possible to extend the effective dynamic range of the controller, while keeping the required quality of attenuation within the bandwidth of the controller. This strategy cannot be implemented with a conventional feedbacked controller working in the time domain. Feedforward controllers are not subjected to the waterbed effect, but can only be used for a detailed plant estimation and a harmonic spectrum constant in time (Akogyeram and Longman, 2001). In this work, a controller that combines the action of both, time and frequency domains, fixing the waterbed effect problem is presented. The used frequency domain algorithm is related to the more sophisticated gradient algorithms (Nelson and Elliot, 1992), and also to higher harmonic control (HHC) or Multicyclic Control (Johnson, 1982; Patt *et al.*, 2005).

The simplification in the proposed method relays in the use of the Fast Fourier Transform (FFT) to extract the information from the measured output signal, necessary to close the control loop using a simple PI

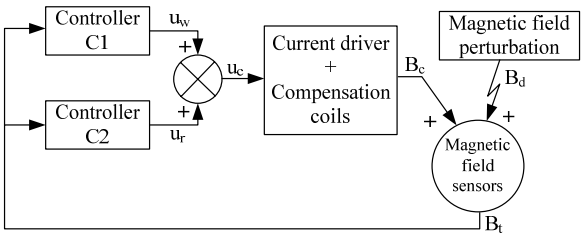

Figure 1: Description of the system

controller. This is an important characteristic of the algorithm since, in the context of the present problem, it is not possible to measure the perturbation alone as it is frequently done in active noise cancellation.

In this manuscript we deal with a magnetic field active shielding system designed for Fast Field Cycling (FFC) Nuclear Magnetic Resonance (NMR) experiments. The experimental situation has already been described in an earlier publication (Forte *et al.*, 2010).

II. CONTROL STRATEGY

Non-periodic disturbances are canceled with a conventional PID controller (C1) working in the time domain. A second PI controller (C2) working in the frequency domain is added to deal with harmonic perturbations (Fig. 1). Controller in the time or frequency domain refers to how is it expressed its input signal (Palani, 2010). While C1 works with the signal as it is measured by the magnetic field sensor, C2 works with its Fourier Transform.

If a harmonic component occurs at a frequency where the waterbed effect manifests for C1, the action of C2 will compensate the effect thus extending the dynamic range of the combined system.

All magnetic fields are time-dependent. For simplicity, it is not included the time dependence (t) of the different magnetic field variables explicitly in the text. The relevant signals affecting the system of Fig. 1 are:

$$B_t = B_d + B_c = B_{rt} + B_{wt} \tag{1}$$

where B_t is the total magnetic field sensed, B_d represent all the disturbances, B_c is the compensating magnetic field, B_{rt} is the f_r frequency component of the total magnetic field and B_{wt} includes all frequency components of B_t different from f_r.

$$B_d = B_{rd} + B_{wd} \tag{2}$$

where B_{rd} is the armonic disturbance that will be cancelled by C2 and B_{wd} represents all other disturbances that will be cancelled by C1.

$$B_{rd}(t) = \widehat{B_{rd}} sin[2\pi f_{rd} t] \tag{3}$$

where $\widehat{B_{rd}}$ is the amplitude of $B_{rd}(t)$ and f_{rd} is the frequency of $B_{rd}(t)$.

$$B_c = B_{rc} + B_{wc} \tag{4}$$

where B_{rc} is the compensation signal generated by C2 and B_{wc} is the compensation signal generated by C1.

$$B_{rc}(t) = \widehat{B_{rc}} sin[2\pi f_{rc} t + \theta_{rc}(t)] \tag{5}$$

where $\widehat{B_{rc}}$ is the amplitude of $B_{rc}(t)$, f_{rc} is the frequency of $B_{rc}(t)$ and $\theta_{rc}(t)$ is the phase of $B_{rc}(t)$ with respect to $B_{rd}(t)$.

For any controller working in harmonic noise mitigation, the solution will be equivalent to the addition of an antiphase signal, with same frequency and amplitude than that of the perturbation. If the parameters ($\widehat{B_{rd}}$ and f_{rd}) of the harmonic perturbation (Eq. 3) are well known, it is possible to eliminate B_{rd} if we do:

$$\widehat{B_{rc}} = \widehat{B_{rd}} \tag{6}$$

$$f_{rc} = f_{rd} \tag{7}$$

$$\theta_{rc} = K_{ri} \int_T |B_{rn}| dt \tag{8}$$

where K_{ri} is a design parameter, T is the control loop period of C2 and B_{rn} is the normalized amplitude of B_{rt} defined as $\frac{B_{rt}}{\widehat{B_{rd}}}$.

If Eqs. 6 and 7 hold, it is possible to find a value of K_{ri} (Eq. 8) that satisfies $\theta_{rc}(t) \to \pi$ when $t \to \infty$. As it is assumed constant (or slowly varying) frequency and amplitude characteristics for the harmonic component of the perturbation B_{rd}, both $\widehat{B_{rd}}$ and f_{rd} can be approximated through a high-resolution FFT before starting the active cancellation process. Once the controllers are fully active, B_{rt} is cyclically calculated trough a fast FFT performed on the samples acquired during the C2 loop period (T).

$$\widehat{B_{rc}} \approx \widehat{B_{rd}} \tag{9}$$

$$f_{rc} \approx f_{rd} \tag{10}$$

$$\theta_{rc} = K_{ri} \int_T i_k |B_{rn}| dt \tag{11}$$

where: k is the control iteration index.

$$i_k = \begin{cases} -i_{k-1} & \text{if } \frac{d\widehat{B_{rt}}}{dt} > \alpha \text{ and } \frac{d^2\widehat{B_{rt}}}{dt^2} > 0 \text{ or} \\ & \text{if } \frac{d\widehat{B_{rt}}}{dt} < -\alpha \text{ and } \frac{d^2\widehat{B_{rt}}}{dt^2} > 0 \\ i_{k-1} & \text{otherwise} \end{cases}$$

α is a design parameter used to introduce a hysteresis in the swith condition of i_k. For the first iteration ($k = 1$) i_k is initilized with 1.

In Eq. 11, the sign of the integral argument is changed every time B_{rt} passes throught a minimum. In this way, it is possible to keep both signals (B_{rd} and B_{rc}) near antiphase, although their magnitude were different. In steady state, the system behaves as an on-off controller, keeping B_{rt} oscillating around their minimum value (amplitude modulation - AM - with

a small depth index). This behavior seems to be a common feature of this kind of controllers (see for instance Sergeant *et al.*, 2007). The amplitude of the oscillation depends on the time interval between the moment at which B_{rt} reaches the minimum, and the change in the sign of the C2 integral argument (Eq. 11). Ideally, if this time interval is reduced to zero, the amplitude of the oscillation cancels (there is no modulation). However, for robustness, it is mandatory to admit a certain hysteresis (like in every on-off controller) by setting $\alpha > 0$.

It is desired that the total magnetic field at f_r frequency never becames larger than the disturbance at the same frequency, that is:

$$B_{rt} < B_{rd} \tag{12}$$

This condition can be expressed in therms of the phase angle:

$$\pi - \frac{\pi}{3} < \theta_{rc} < \pi + \frac{\pi}{3} \tag{13}$$

Which implies that it must be satisfied that:

$$K_{ri} \int_T |B_{rn}| dt < \frac{\pi}{3} \tag{14}$$

As B_{rn} is normalized, its maximum possible value is 2 (when B_{rc} and B_{rd} are in phase). Then,

$$K_{ri} T 2 < \frac{\pi}{3} \Rightarrow K_{ri} < \frac{\pi}{6T} = K_{ri_{max}} \tag{15}$$

Now, if the disturbance frequency suddenly change, making $f_{rd} \neq f_{rc}$ while the amplitude does not suffer any change, the envelope of the sum of $B_{rc} + B_{rd}$ will be:

$$\text{envelope of } B_{rc} + B_{rd} = 2A \; sin(\frac{|f_{rc} - f_{rd}|}{2} t) \tag{16}$$

where $A = \widehat{B_{rc}} = \widehat{B_{rd}}$.

Using Eq. 16, to preserve inequality 12, it must be satisfy that:

$$T < \frac{2}{d_f} asin(\frac{1}{2}) \Rightarrow T < \frac{\pi}{3 d_f} \tag{17}$$

$d_f = |f_{rd} - f_{rc}|$.

Since the dynamics of the plant is intrinsically driven by the control algorithm of C2, the command signal u_c applied to the plant will just depend on the gain K_p of the plant transfer function:

$$u_c = K_p^{-1} * B_{rc} \tag{18}$$

where K_p is the gain of the plant transfer function.

Controllers C1 and C2, do not affect their performance each other. C1 can only modify the magnitude of the disturbance view by C2, but in steady way over time. In addition, C1 views the magnetic field generated by C2 as any other perturbation.

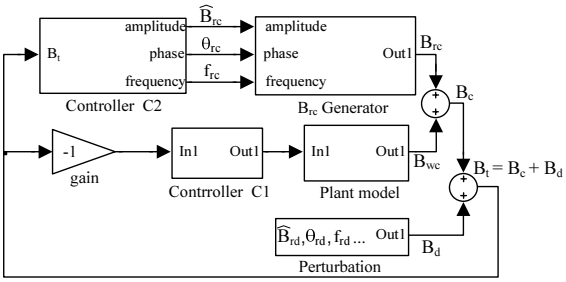

Figure 2: Simulation model: general diagram.

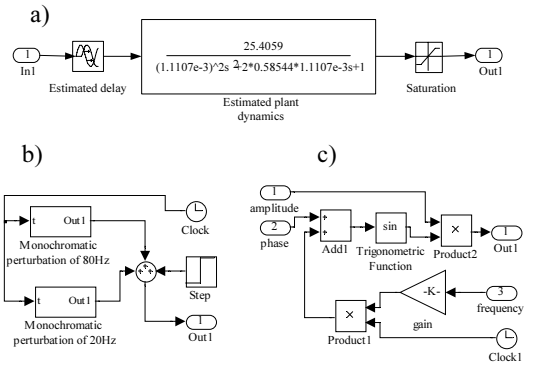

Figure 3: Details inside blocks of Fig. 2: a) Plant model. b) Perturbation (with two frequency harmonic components and offset) and c) B_{rc} generator.

III. SIMULATED ALGORITHM PERFORMANCE TESTS

The algorithm was applied to a controller aimed for a magnetic field active shielding (Forte *et al.*, 2010). The controlled variable $B_c(t)$ is the mean magnetic field along one axis direction. The actuator consists of a set of coils generating a homogeneous magnetic field along the same axis of $B_r(t)$. The current flowing through these coils are handled by the combined action of controllers C1 and C2. The plant is modeled by a second order transfer function with delay:

$$G(s) = \frac{K_p e^{-sT_p}}{\omega^2 s^2 + 2\xi\omega s + 1}, \tag{19}$$

where $G(s)$ is the transfer function in the Laplace domain (s), T_p is the time delay [s], ξ is the damping factor and ω is the natural frequency [r/s].

The transfer function parameters values are: $K_p = 25.54$, $T_p = 510\text{e-}5$, $\xi = 0.647$ and $\omega = 1.4\text{e-}3$ (Forte *et al.*, 2010).

Simulations were carried out using the Simulink toolbox of MatLab. A general block-scheme of the system can be observed at Fig. 2. The plant has been modeled with a linear transfer function of second order, including delay and a saturation block represent-

ing the largest current output allowed by the hardware (Fig. 3a). As an example, it can be considered here the case where the system has to deal with a perturbation composed of two definite frequency components and an offset (Fig. 3b).

C1 attenuates constant disturbances and one of the harmonics (with its frequency defined within the bandwidth of the controller). A compensating signal was added to cancel the second harmonic, with frequency defined within the range where the waterbed effect dominates the response of the C1 controller. This signal is generated by the subsystem shown in Fig. 3c and it is managed by the specifically designed controller C2.

The input signal to the C1 controller is the error e defined as follows:

$$e(s) = r(s) - c(s) \tag{20}$$

where c is the controlled variable and r is the reference signal.

The purpose of the control is to cancel the magnetic field, that is, $e(s) = -c(s)$. The PID controller equation (Ziegler and Nichols, 1942) is:

$$u_w(s) = K_w \left[1 + \frac{1}{T_{iw}s} + T_{dw}s\right] e(s) \tag{21}$$

where $u_w(s)$ is the controller output and the plant input and K_w, T_{iw} and T_{dw} are the parameters of the controller.

The controller was tuned following the Sung method (Sung *et al.*, 1998) (K_w = 13.6e-3, T_{iw} = 2.7 and T_{dw} = 1.5e-3). Simulations were done by discretization (Ogata, 1987).

When the frequency domain controller C2 is turned on, a FFT with a large number of samples is performed to determine the amplitude and frequency of the perturbation (B_{rd} and f_{rd}). During this step, both controllers are inoperative. Once the system is fully working, a faster FFT (few samples) is cyclic performed to close the loop of the phase-tracking procedure. The subsystem that tracks the phase, integrates all the time the amplitude component of the resulting magnetic field $B_{rc}(t) + B_{rd}(t)$ at f_{rc} frequency. This feedback signal is normalized dividing it by $\widehat{B_{rd}}$, in order to keep the loop gain independent of the perturbation intensity.

Parameters of controller C2 were set as follow: Sample frequency $f_s = 1KHz$, control loop period $T = 64ms$, $K_{ri} = 5 < \pi/(6 * T)$. So, the largest possible change of the disturbance frequency during T is: $d_{f_{max}} = \pi/(3 * T) = 16.4Hz$.

The most important block of this controller is that checking the sign of the integral argument, used to define the sign of the phase step of $\theta_c(t)$. The decision of switching from phase increment to phase decrement (or vice versa) is taken in the moment at which the perturbation intensity crosses a minimum (see Fig. 4). A

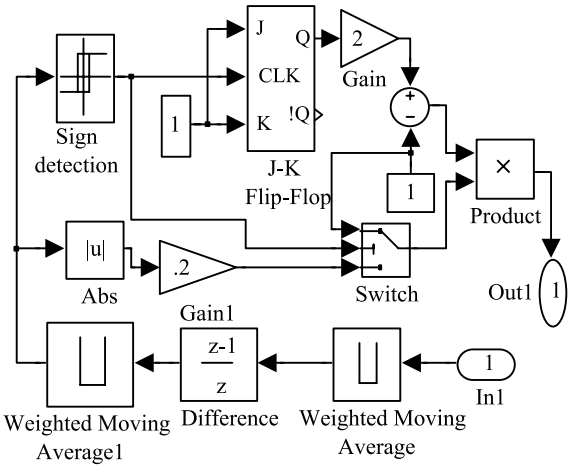

Figure 4: Details of the block involved in the minimum intensity condition detection for the phase-tracking algorithm.

moving average filter is applied before and after calculating the derivatives. A J-K flip-flop managed by the sign of the previously calculated derivative detects the condition of passing through a minimum. At the end of this block, the output is multiplied by the absolute value of the derivative, only when B_{rt} is decreasing in time.

Initially, C1 was tested with two frequency components ($20Hz$ and $80Hz$), one within the bandwidth of the controller, and the other in the range where the PID amplifies. Frequencies beyond the limit imposed by the sample rate will be rejected by the antialiasing filter and will not be affected by the system (Oppenheim *et al.*, 1983). In turn, a step was added at t = 3.5s. As expected, the low-frequency component is attenuated while the other is amplified. The C1 controller behaves satisfactorily with the step perturbation, which drives it to zero immediately. The same perturbation was later applied to C2. Since the algorithm was designed to cancel only one frequency component (the highest), C2 attenuates that component without affecting the other. However, the step is not affected by this controller.

Figure 5 shows the simulated result when both C1 and C2 are working simultaneously. At t = 2.5s C2 starts attenuating the perturbation using the information recovered until that time. C1 is turned on at t = 3s. Two small lateral bands arise around the frequency component of $80Hz$ as a consequence of the AM modulation effect of the C2 controller. The total disturbance spectral energy is conveniently reduced when both controllers are working.

IV. EXPERIMENTAL

Experiments were carried out using the platform already described in Forte *et al.*, 2010. A new dedicated

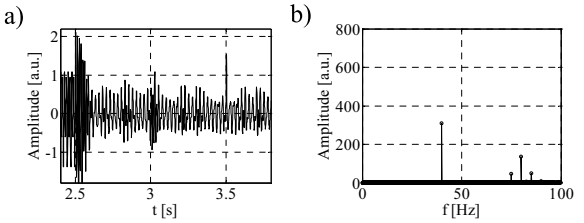

Figure 5: a) Total magnetic field when both controllers are active. At time t=3.5s a step perturbation is introduced. b) Spectrum of the magnetic field after the step perturbation have been added.

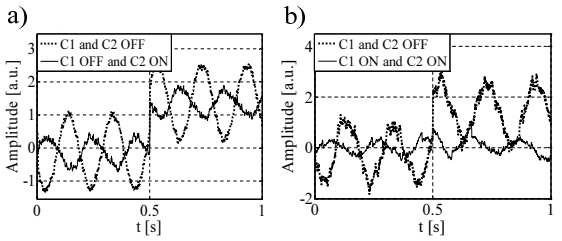

Figure 6: a) The controller C2 can attenuate a harmonicu perturbation but has no effect if a step is introduced. b) The combination of both controllers (C1 and C2) results in a system that con diminishes both kinds of perturbations.

hardware executes the control tasks that were previously based on PC environment. The system is based on a TMX320F28335 digital signal controller (DSC). The magnetic field feedback information is read from the hall sensors using two MAX1316 analogue to digital converters (ADC), providing 10 input channels. The controller also has 8 analogue outputs provided by two DAC8544 digital to analogue converters (DAC), used to manage the currents flowing through the compensating coils. Data are moved between ADCs and the DSC by direct memory access (DMA) thus optimizing the system speed. The control loop sample time is governed by an internal timer which reduces the hitter to the minimum. This issue critically affects the performance of the controller, being however this a minor problem at the present stage of concept testing.

As a first experiment, the frequency response of C1 was characterized. The waterbed effect starts to manifest at a frequency of about 10Hz. In contrast to C1, controller C2 does not have a region where disturbances are amplified, but if a step is applied, this controller has no effect (Fig. 6a). The two controllers have been lump together resulting in a system with good frequency characteristics and capability of step compensation (Fig. 6b). Experiments of Fig. 6 were done with a perturbation having its frequency within the bandwidth of C1. Figure 7 shows that the negative effect of C1 at a frequency where the waterbed effect dominates, can be practically eliminated by the action of C2, when both controllers are working.

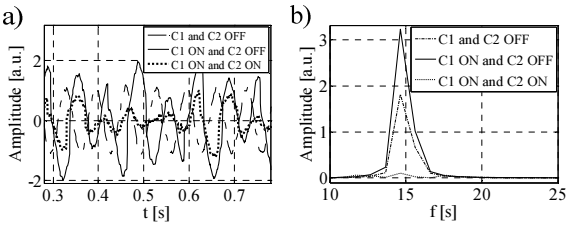

Figure 7: System behavior for a perturbation of frequency where C1 acts as an amplifier. a) Time domain signals. b) Spectral representation.

V. DISCUSSION

A deficiency of the proposed solution is related to the phase-tracking algorithm. A hysteresis is introduced from the determination of the sign of the phase steps (increments or decrements) which is based on the calculation of derivatives. As this operation is highly sensibly to noise, the controller changes the sign of the feedback signal before B_{rt} passed through its minimum value. This situation would produce a momentarily loss of control, resulting in an undesirable peak in B_{rt} (of magnitude $\widehat{B_{rc}+B_{rd}}$). The added hysteresis demands checking that $\mathrm{d}B_{rt}/\mathrm{d}t$ remains positive for a while after crossing the minimum.

The amplitude and frequency of the compensating signal differ from the real disturbance due to unavoidable errors of the FFT. The controller must be constantly tracking the phase of $B_{rd}(t)$ to cancel the harmonic perturbation, thus imposing a frequency limit for the algorithm loop. Moreover, every control loop, the FFT of $B_t(t)$ is performed to measure the feedback signal. This FFT should have the minimum quantity of samples needed to characterize B_{rt}, also affecting the frequency response of the controller. Therefore, the algorithms used to measure the frequency and amplitude of the perturbation and the phase-tracking procedure, are critically affecting the dynamic range of the system. This drawback could be overcame by sensing the perturbation outside the exclusion volume and using a feedborward controller. However, in our application, the surroundings of the exclusion volume are affected by the time dependent disperse field of the main magnet of the relaxometer.

Unlike other control strategies, like repetitive control (Hara *et al.*, 1985) or iterative learning control (Arimoto *et al.*, 1986), the simple method proposed in this work can selectively reject harmonic perturbations. This is an important issue when, at the output of the system, the perturbation contains harmonic components that should remain unaffected. Existing

control strategies for the rejection of harmonic components are based on the estimation of the main component (see for example Bodson *et al.*, 2001). In this work, every control cycle the systems seeks perturbation information, thus avoiding the risk that the estimator does not converge. If for any circumstance, the controller looses the control of the antiphase signal, the system recovers itself after a transient time where the perturbation can be amplified at most by a factor of two.

VI. CONCLUSIONS

It was shown that the waterbed effect associated to controlled signals in the time domain can be circumvented with the addition of a conventional PI controller working in the frequency domain. In this way, the dynamic range and the performance of the combined controller can be improved. A deeper mathematical analysis is needed to explore the limits of operation, particularly analyzing other alternatives to the FFT and the phase-tracking algorithms. The present scheme can be adapted for the selective rejection of two or more harmonic components, particularly in the case of steady conditions. Experimental results depicted in Fig. 7 clearly shows that the practical implementation of the proposed solution, although involving very simple control concepts, can be extremely efficient.

ACKNOWLEDGEMENTS

The Authors acknowledge the financial support from MINCYT Córdoba, SECyT-UNC and CONICET. We thank to B. Reyes, W. Salinas and F. Barra for the collaboration in the implementation of the new hardware.

REFERENCES

Akogyeram, R. A. and R. W. Longman, "On the choice of the method to cancel 60Hz disturbances in the beam position and energy," *Proceedings of the 2001 particle acelerador conference, Chicago, EEUU*, 1270-1272 (2001).

Anoardo, E. and G. Ferrante, "Magnetic Field Compensation for Field-Cycling NMR Relaxometry in the ULF Band," *Appl. Magn. Reson.*, **24** , 85-96 (2003).

Arimoto, S., S. Kawamura and F. Miyazaki, "Convergence, stability and robustness of learning control schemes for robot manipulators," *Proceedings of the International Symposium on Robot Manipulators on Recent trends in robotics: modeling, control and education*, 307-316 (1986).

Bodson, M. and S. C. Douglas, "Adaptive algorithms for the rejection of sinusiodal disturbances with unknown frequency," *Automatica*, **33**, 2213-2221 (1997).

Bodson, M., J. S. Jensen and S.C. Douglas, "Active noise control for periodic disturbances," *IEEE Transactions on control systems technology*, **9**, 200-205 (2001).

ter Brake, R. Huonker and H. Rogalla, "New results in active noise compensation for magnetically shilded rooms," *Meas. Sci. Technol.*, **4**, 1370-1375 (1993).

Brown, L. J. and Qing Zhang, "Periodic disturbance cancellation with uncertain frequency," *Automatica*, **40**, 631-637 (2004).

Forte, G. O., G. Farrher, L. R. Canali and E. Anoardo, "Automatic Shielding-Shimming Magnetic Field Compensator for Excluded Volume applications," *IEEE Transactions on control systems technology*, **18**, 976-983 (2010).

Hara, S., T. Omata and M. Nakano, "Synthesis of repetitive control systems and its application," *Proceedings of the 24th conference on decision and control*, 1387-1392 (1985).

Johnson, W., *Self-tuning regulators for multicyclic control of helicopter vibration*, National Aeronautics and Space Administration, Scientific and Technical Information Branch, Washington, D.C (1982).

Kimmich, R. and E. Anoardo, "Field-cycling NMR Relaxometry," *Progress in nuclear magnetic resonance spectroscopy*, **44**, 257-320 (2004).

Kuo, S. M. and D. R. Morgan, "Active noise control: a tutorial review," *Proc. IEEE*, **87**, 943-973 (1999).

Kuriki, S., A. Hayashi, T. Washio and M. Fujita, "Active compensation in combination with weak passive shielding for magnetocardiographic measurements," *Rev. Sci. Instrum.*, **73**, 440-445 (2002).

Lurie, D. J., M. A. Foster, D. Yeung and J. M. S Hutchinson, "Design, construction and use of a large-sample field-cycled PEDRI imager," *Physics in Medicine and Biology*, **43**, 1877-1886 (1998).

Matter, N. I., G. C. Scott, T. Grafendorfer, A. Macovski and S. M. Conolly, "Rapid polarizing field cycling in magnetic resonance imaging," *IEEE Transactions on Medical Imaging*, **25**, 84-93 (2006).

Nelson, P. A. and S. J. Elliot, *Active control of sound*, Academic Press, San Diego (1992).

Ogata, K., *Discrete-Time Control Systems*, Prentice Hall, Upper Saddle River, New Jersey (1987).

Oppenheim, A. V., A. S. Willsky and I. T. Young., *Signals and systems*, Prentice Hall, Englewood. Cliffs, New Jersey (1983).

Palani, S., *Control Systems Engineering,* Tata McGraw Hill, New Delhi (2010).

Patt, D., L. Liu, J. Chandrasekar, D. S. Bernstein and P. P. Friedmann, "Higher-Harmonic-Control Algorithm for Helicopter Vibration Reduction Revisited," *Journal of guidance, control, and dynamics*, **28**, 918-930 (2005).

Platzek, D., H. Nowak, F. Giessler, J. Röther and M. Eiselt, "Active shielding to reduce low frequency disturbances in direct current near biomagnetic measurements," *Rev. S. Instrum.*, **70**, 2465-24709 (1999).

Sergeant, P., L. Dupré, M. De Wulf and J. Melkebeek, "Optimizing Active and Passive Magnetic Shields in Induction Heating by a Genetic Algorithm," *IEEE Trans. Magn.*, **39**, 3486-3496 (2003).

Sergeant, P., A. Van Den Bossche and L. Dupré, "Hardware control of an active magnetic shield," *IET Sci. Meas. Technol.*, **1**, 152-159 (2007).

Skogestad, S. and I. Postlethwaite, *Multivariable feedback control. Analysis and Design*, John Wiley and Sons, Ltd., Chippenham, Wiltshire (2005).

Sung, S. W., I. B. Lee and J. Lee, "New process identification method for automatic design of PID controllers," *Automatica*, **24**, 513-520 (1998).

Ziegler, J. G. and N. B. Nichols, "Optimum settings for automation controllers," *Transactions of the ASME*, **64**, 759-768 (1942).

Received: June 28, 2011.
Accepted: May 4, 2012.
Recommended by Subject Editor José Guivant.